Article

Reusability Comparison of Melt-Blown vs. Nanofiber Face Mask Filters for Use in the Coronavirus Pandemic

Sana Ullah, Azeem Ullah, Jaeyun Lee, Yeonsu Jeong, Motahira Hashmi, Chunhong Zhu, Kye Il Joo, Hyung Joon Cha, and Ick-Soo Kim

Just Accepted

Reusability Comparison of Melt-Blown vs. Nanofiber Face Mask Filters for Use in the Coronavirus Pandemic

Sana Ullah[α‡], Azeem Ullah[α‡], Jaeyun Lee[β‡], Yeonsu Jeong[β‡], Motahira Hashmi[α], Zhu Chunhong[£], Kye Il Joo[β], Hyung Joon Cha[β]*, and Ick Soo Kim[α]*

[α]Nano Fusion Technology Research Group, Institute for Frontier Fibers, Shinshu University, Ueda campus, Nagano, 386-0017, Japan

[β]Department of Chemical Engineering, Pohang University of Science and Technology, Pohang 37673, Korea

[£]Faculty of Textile Science & Technology, Shinshu University, Ueda campus, Nagano, 386-0017, Japan

*Corresponding authors: Hyung Joon Cha, hjcha@postech.ac.kr; Ick Soo Kim, kim@shinshu-u.ac.jp

[‡]S. Ullah, A. Ullah, J. Lee, and Y. Jeong have equal contribution in this research.

1

Abstract

Shortage of face masks is a current critical concern since the emergence of coronavirus-2 or SARS-CoV-2 (COVID 19). In this work, we compared the melt-blown (MB) filter, which is commonly used for the N95 face mask, with nanofiber (NF) filter, which is gradually used as an effective mask filter, to evaluate their reusability. Extensive characterizations were performed repeatedly to evaluate some performance parameters, which include filtration efficiency, airflow rate, and surface and morphological properties, after two types of cleaning treatments. In the first cleaning type, samples were dipped in 75% ethanol for a predetermined duration. In the second cleaning type, 75% ethanol was sprayed on samples. It was found that filtration efficiency of MB filter was significantly dropped after treatment with ethanol, while the NF filter exhibited consistent high filtration efficiency regardless of cleaning types. In addition, the NF filter showed better cytocompatibility than that of the MB filter, demonstrating its harmlessness on the human body. Regardless of ethanol treatments, surfaces of both filter types maintained hydrophobicity, which can sufficiently prevent wetting by moisture and saliva splash to prohibit not only pathogen transmission, but also bacterial growth inside. Based on these comparative evaluations, it is highly recommended the wider use of the NF filter for face mask applications, which can be reused multiple times with robust filtration efficiency. It would be greatly helpful to solve the current shortage issue of face masks and significantly improve safety for front line fighters against coronavirus disease.

Keywords: coronavirus; face mask; nanofiber filter; melt blown filter; reusability; cell study; filtering efficiency

Introduction

Since the emergence of the new type of coronavirus (COVID-19 hereafter), the number of infected

persons is increasing exponentially. According to the World Health Organization (WHO), 6,663,

304 cases of COVID-19 has been reported until June 6, 2020. (1) There are limited data on clinical

characteristics of COVID-19; some of the researchers claimed a 4.3% mortality rate while others

claimed less. (2,3) Some of the major symptoms and parameters have been reported to investigate

the presence of COVID-19 in a patient. (4) Since the first infection reported in early December

2019, there have been extensive studies about the origin, symptoms, trend of infection, the

transmission of infection from person to person, possible preparation of vaccine (which has not

yet prepared successfully by any of the researchers), and precautionary measures. (5–14) Some

researchers claimed that coronavirus can be inactivated by heat using the N95 face mask, which is

known to be one of best face masks but is limited to one-time use only. (8)

Personal protective equipment (PPEs) became a hot issue since the emergence of COVID-19

pandemic. Because there is no possible vaccine at this time, PPEs are a major concern in fighting

against this pandemic. Even higher authorities and institutions including WHO is concerned about

the shortage of face masks suggesting the public use cloth masks even if medical masks are not

available in markets. China is a major producer of face-masks with almost 50% contribution in

global face-masks consumption. (15) However, it is clear that COVID-19 has badly affected the

production and supply of face-masks throughout the world. Countries having the capacity of

producing face-masks are also suffering from a shortage of face-masks. These countries include

developed nations like the European Union, U.S.A, Japan, and the U.K. N95 is one of the best

available filters so far but it is limited to single-use only. It was reported that COVID-19–can

survive for a week on the outer surface of the face-mask. That makes it complimentary to proper

treatment before reuse or even for disposal of face-masks. However, current studies have been done to sterilize N95 filter-based face-masks using UV light. (16) In general, the N95 filter is produced by melt-blown (MB) process. Studies also show that common fabrics may have filtering efficiency of 80%-95% depending on fabric structures. (17–19)

It was reported about the investigation on the effect of nano treatment (treatment by nano functional materials such as nanoparticles) on the N95 and surgical masks subjected to thermo-physiological responses and discomfort. (20) They reported that subjects wearing nano-treated surgical masks have significantly lower heart rates. The outer surface temperature of the nano-treated surgical masks was higher than that of the N95 masks. However, micro-environment and skin temperatures were lower in the nano-treated surgical masks. Furthermore, N95 masks reported having significantly higher absolute humidity inside the mask surface. All nano-treated surgical masks were reported to have a significantly lower perception of heat, humidity, and overall discomfort. (20) There was a study on the protective performance of N95 and surgical face masks. They reported that N95 masks had significantly lower air permeability and water vapor permeability than surgical masks. *In vivo* test revealed that N95 masks can filter out 97% of the foreign bodies while surgical masks can be as good as up to 95%. Nano-treated surgical masks can provide additional protective functions in stopping capillary diffusion and antibacterial activities. (21) Study was basically conducted to investigate N95 protection against the airborne viruses *versus* surgical masks. (22) They reported that N95 filtering masks may not provide the expected protection level against significantly small but are much more efficient than the surgical masks against the infection causing agents in the range of 10–80 nm. There was a survey on the risks involved in causing headaches due to wearing N95 respirators.(23) They reported that due to higher humidity levels, breath resistance, and accumulation of heat inside the micro-climate of the

masks result in headaches. Thus, they suggested shorter duration of masks wearing can significantly reduce the severity of the headaches. It was also conducted a survey on the protection level of the surgical masks *versus* N95 masks for preventing influenza among the health care workers. (24) They reported that N95 masks were not better in protection against influenza than the surgical masks.

Electrospun nanofibers have a wide range of applications in healthcare, (25–30) environmental engineering, (31,32) and energy storage sectors. (33) Currently, nanofibers are being produced in bulk quantity in some countries including Korea, Japan, the U.S.A, and European countries. Nanofibers are the best replacement for microfibers and thin films due to their distinct features including the higher surface area which can be functionalized for desired the property, uniform morphology, consistency in structural properties, and simple technique to fabricate nanofibrous mats. Thus, nanofiber filters are gradually used for mask applications in the world. In the present work, we performed a comparative study on the performance properties of MB (N95) and nanofiber-based air filter masks for evaluation on reusability after cleaning (spraying and dipping) using 75% ethanol by determinations of air permeability, surface area, porosity, morphological properties, and filter performance (**Figure *1***).
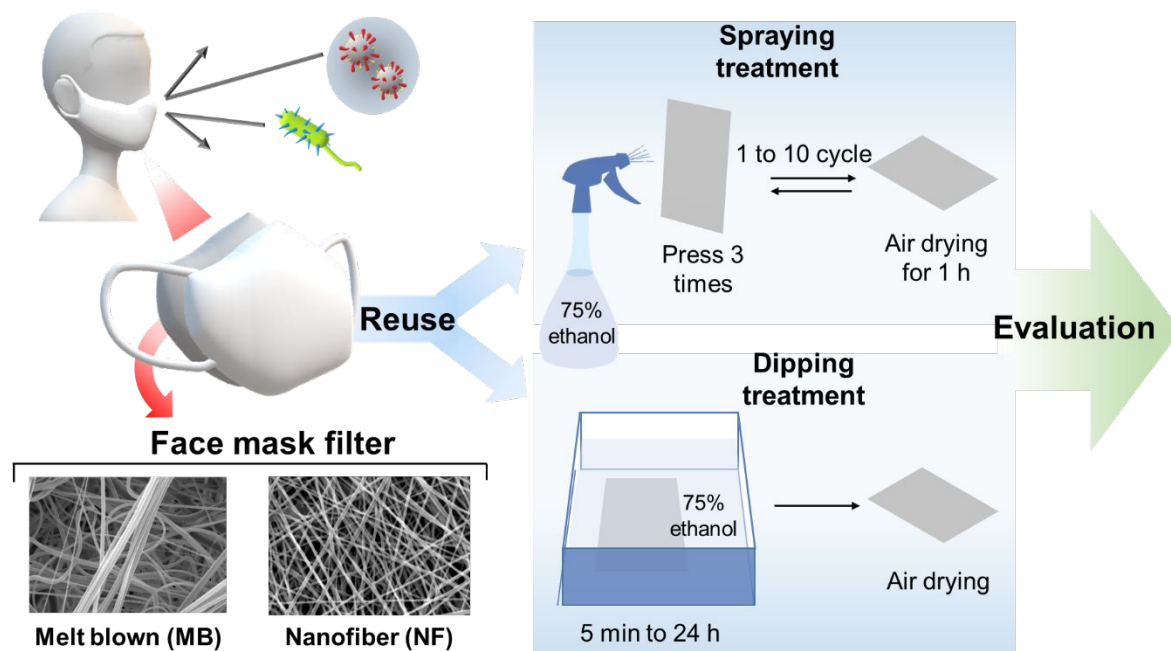
Figure 1 Schematic diagram on spraying and dipping treatments of face mask filters using 75% ethanol for evaluation of reusability.

Results and discussions

Physicochemical study

FTIR spectra of the MB and NF filters are shown in **Figure 2**. In the FTIR spectrum of MB filter confirm the polypropylene composition of the MB filter, the peak at 2922 cm^{-1} represented the CH$_2$ group vibration in main PP polymer chain. The spectrum also showed four peaks in the wavelength range of 3000 cm^{-1} and 2800 cm^{-1}; the peaks at 2955 cm^{-1} and 2873 cm^{-1} can be attributed to CH$_3$ asymmetric and symmetric stretching vibrations, while the peaks at 2922 cm^{-1} and 2843 cm^{-1} were due to CH$_2$ symmetric and asymmetric vibrations, respectively. (34) The intense peaks at 1478 cm^{-1} and 1360 cm^{-1} were caused by the CH$_2$ scissor vibrations or CH$_3$ symmetric and asymmetric deformation vibrations. PP FTIR spectrum showed characteristic

fingerprint peaks in the region of 1200–750 cm^{-1}. These peaks can be attributed to C-C as symmetric stretching, CH$_3$ asymmetric rocking, and C-H wagging vibrations and CH$_2$ rocking vibrations. (34,35) In the spectra of the NF filter, the FTIR spectrum of spun bond PET side showed an intense peak 1704 cm^{-1} which is a characteristic of C=O symmetric stretching and also these stretching can be seen at wavenumber 1257 cm^{-1}. The moderate C-H stretching can be seen at 2947 cm^{-1}. A very weak peak at 3437 cm^{-1} was attributed to the -OH group bonded to C=O. The peak at 983 cm^{-1} can be attributed to the out of plane bending of the -OH group in PET chains. The peaks observed at 1250–950 cm^{-1} are assigned to C-C stretching and C-H in plane bending in PET polymer chain. (36) The peaks at 1431 cm^{-1} can be attributed to C − H deformation in the PVDF polymer chain. (37) The peak at 869 cm^{-1} was attributed to α crystal of the PVDF.[38] The peak at 1177 cm^{-1} was attributed to the C-F stretching's. (39)
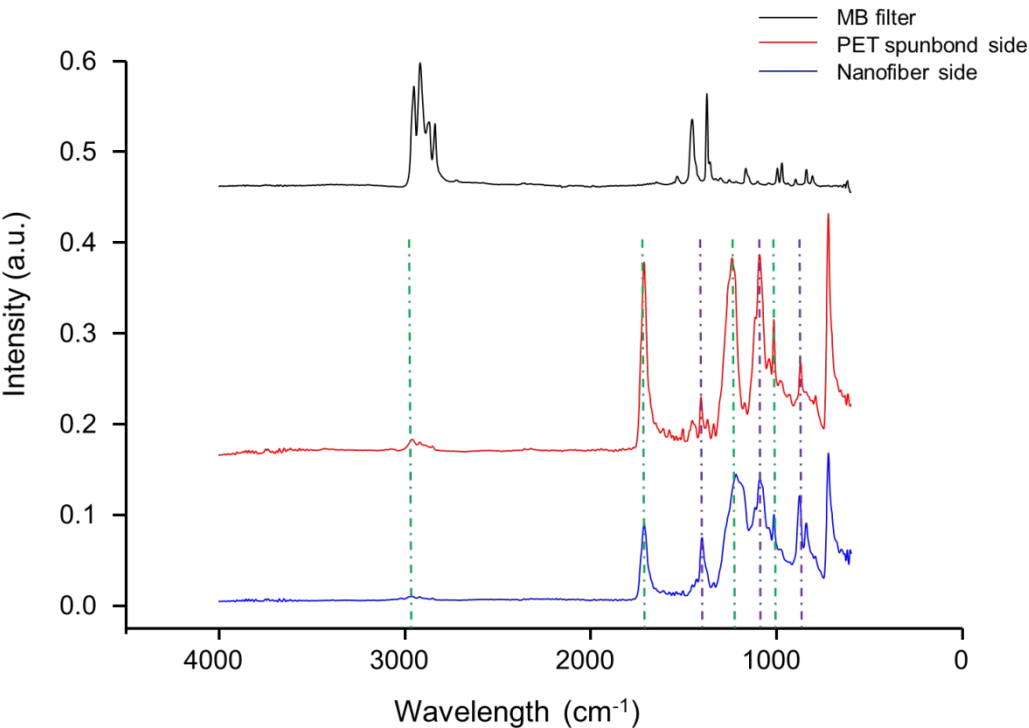
Figure 2 FTIR-ATR spectra of MB filter, and NF filter (both sides; Nanofiber and spun bond sides): FTIR spectra confirm the polypropylene composition of the MB filter while PET and PVDF composition in NF filter

Evaluation of filter performance

To evaluate reusability of MB and NF face mask filters, we used two types of cleaning procedures including 75% ethanol spraying up to 10 cycles (1 cycle is 3 times press of sprayer) and dipping in 75% ethanol. All possible parameters were considered for comparative characterizing the performance of MB and NF filters before and after cleaning with ethanol. First, air permeability (air flow rate) of both filters were measured (**Figure 3a**). It was observed that air permeability (in cfm unit) of MB filter was recorded ~27.2 cfm as an average value before ethanol treatment. However, there was not a significant difference noted after ethanol treatment regardless of cleaning types. In the case of the NF filter, air permeability was about 17.0 cfm before cleaning but slightly decreased after ethanol treatment. Because the PVDF-based NF filter in this work was supported by spun-bond polyethylene terephthalate (PET), it may be one of the possibilities that when the NF filter was treated with ethanol, PET could be depolymerized to diethylene or mono-ethylene. While 100% depolymerization of PET is only possible in supercritical conditions, partial depolymerization is possible. (40,41) Thus, partial depolymerization of PET might make NF filter more flatter rather than round, decreasing pore size through changing in the morphology of spun-bond PET. Thus, it can be concluded MB filter does not have a significant effect on air permeation by ethanol treatment, however, the NF filter exhibited slightly lower air permeability after ethanol treatment.

Next, the pressure drop was investigated to analyze inhaling/exhaling difficulties which are dependent on porous structure, morphology, and construction of each filter. It was observed that

8

the pressure drop for the MB case was lower than the NF filter (**Figure 3b**). In the case of the MB filter, there was no significant pressure drop when treated with ethanol. However, while the pressure drop of the NF filter was increased when treated with ethanol, it was within limits of safe use. (42) Because PET is not stable in ethanol, its partial depolymerization might lead the NF filter to resist more air, simultaneously making it a little non-uniform. However, at this stage of the study, nothing can be claimed. It needs to be investigated further for a possible mechanism of increased pressure drop in the case of ethanol-treated PET.

Breathing comfort is also dependent on rate of moisture transportation through the filter. Breathability test was performed to evaluate WVTR (**Figure 5b**). It was observed that WVTR of NF filter was superior to that of MB filter. There might be two possible reasons. First, because MB filter has sponge-like structure which resists moisture hence it will take longer time to pass through the filter. However, NF filter has finer structure, uniform morphology, and uniform pore diameter which allow the water vapors to be passed through the filter more efficiently. Second, while pressure drop and efficiency test where NaCl particles were used according to ASTM standard, but in case of WVTR, there was no salt present in water. Because NaCl particle size is larger than pore diameter of NF filters, pressure drop was recorded higher in case of NF filter. However, water vapor has smaller particle size which can easily pass through both filters. It was also reflected in results of efficiency test that NF filter exhibited consistent efficiency due to uniform pore structure while MB filter's efficiency was dropped in result of ethanol treatment. Concluding performance properties; pressure drop and air permeability were found better in case of MB filter however breathability results were opposite. Thus, pressure drop is not a direct indication of breathing comfort or discomfort. As for pressure drop measurement NaCl particles are used which have larger particle size as compared to that of air, so pressure drop cannot be basis of breathability.

WVTR results also confirmed that breathing performances of both types of filters was sufficient
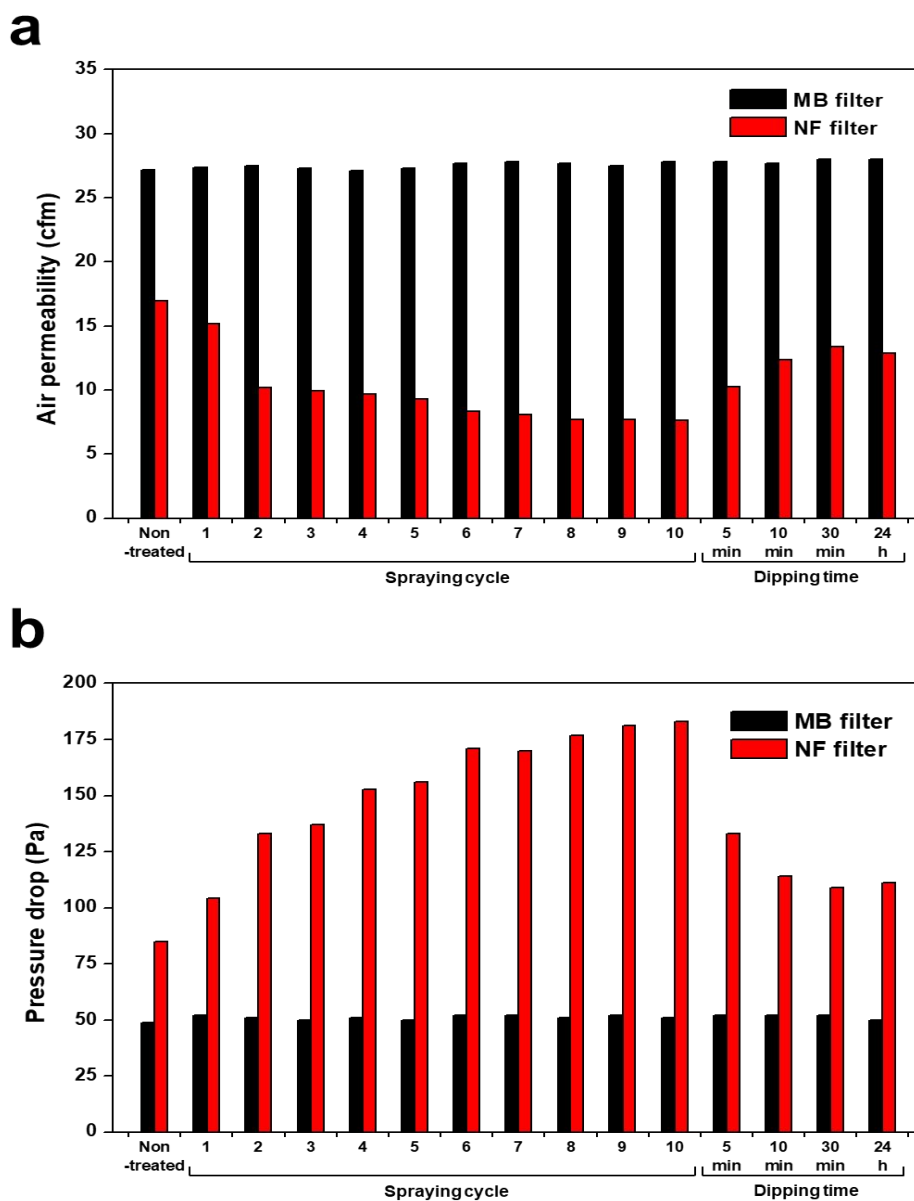
for practical use.

a

b

Figure 3 (a) Air permeability and (b) pressure drop for MB and NF face mask filters before and after spraying and dipping treatments using 75% ethanol

10

Filtration efficiency is one of the major concerns when it comes to face mask performance criteria. Thus, the filtration efficiency test was also performed to investigate the validity of reuse (**Figure 4**). We found that the filtration efficiency of MB filter was significantly dropped to ~84% and ~62% after ethanol spraying with 1 cycle and 10 cycles, respectively (**Figure 4a**). Similar to spraying treatment, filtration efficiency of MB filter was dropped to ~82% after 5 min and ~65% after 24 h ethanol dipping (**Figure 4b**). Thus, the significant reduction of filtration efficiency of MB filter after ethanol cleaning can lead to a clear conclusion that MB filter which is being used in high rated face masks such as N95 is the best available option for single-use only but it not capable of being reused for face mask applications. Note that we observed disappearing of static surface charge of MB filter after ethanol treatment (**Figure 5a**). This disappearing of static charge is one of the possible reasons that the filtration efficiency of the MB filter was decreased when treated with ethanol. Actually, it was already known that the filtration efficiency of the MB filter is somehow dependent on the static charge on its surface. (43) We also confirmed that the original NF filter does not have any static charge on its surface**.** Importantly, the filtration efficiency of the NF filter had a consistent value of around 98% regardless of ethanol treatment type (**Figure 4**). The maintenance of the filtration efficiency of NF filter might be explained from its filtration mechanism using particle size difference without using static charge.
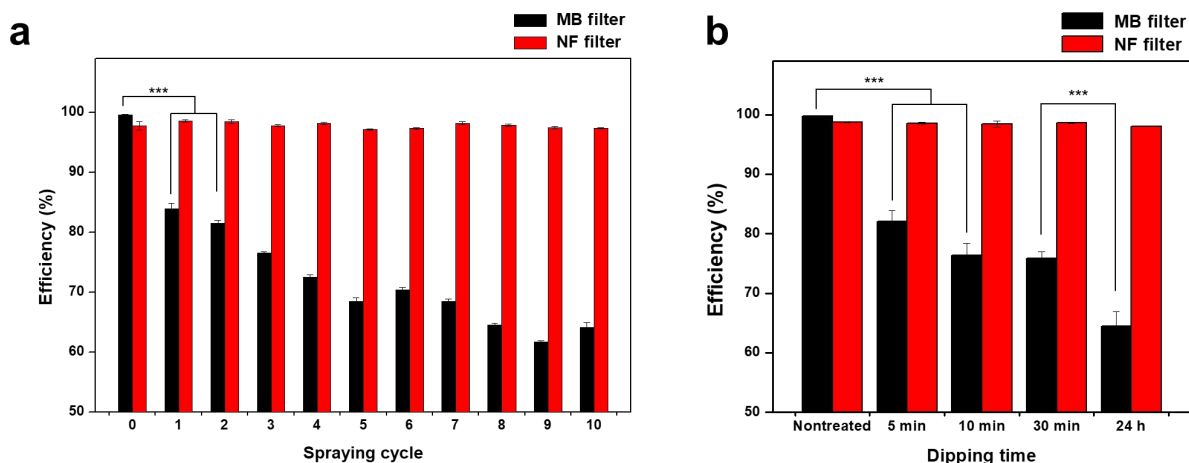
Figure 4 Filtration efficiency of MB and NF face mask filers according to (a) cycle numbers in spraying treatment and (b) time of dipping treatment. The values and error bars represent the means ± standard deviations of at least 3 samples with statistical significance from Student`s unpaired t-test (***p < 0.005).

Figure 5 (a) Observation of static charge on the surfaces of MB and NF face mask filters, and (b) water vapor transport rate of MB and NF filters

12

In addition, we observed that MB filters took more time (about 3 h) to be fully dried while NF filters were dried quickly within 10 min (data not shown). Considering the recent pandemic into account, drying t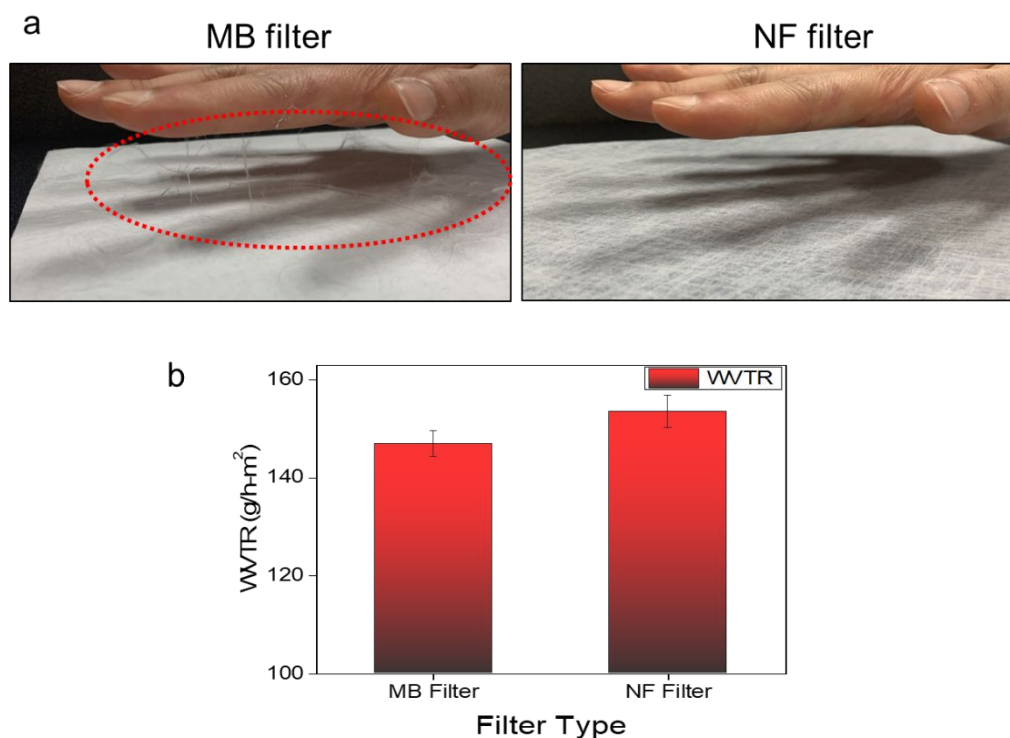ime will also be an important factor because some studies reported that MB filter-based N95 mask gives a favorable environment to viruses and bacteria due to its moisture-loving nature. (22)

Besides air permeation and pressure drop, mask filters should possess breathing comfort features for wearers. Thus, transmissions of air, moisture, and carbon dioxide (CO_2) were evaluated using an infrared thermal camera. It was clearly observed that the NF filter exhibited superior breathing comfort with good thermal behavior to MB filter (**Figure 6a**). NF filter possesses uniform morphology having fine pore diameter (50-100 nm) which is larger than the particle size of air (~4 nm) but smaller than foreign matters including bacteria and viruses (i.e., the particle size of coronavirus is in the range of 80-160 nm). (44) Uniform pore diameter distribution of the NF filter can be one of the possible reasons for good breathing comfort as well as higher and consistent filtration efficiency. In the case of MB filter, diameter distribution was wider due to its non-uniform morphology that can be a possible reason for thermal discomfort and a barrier in the transmission of CO_2 and foreign matters as well. **Figure 6b** shows CO_2 emission mechanism of both types of filters. It can be observed that MB filter exhibited poor emission as compared to that of NF filter. It can be due to sponge like structure, higher thickness, and non-uniform pore diameter of MB filter. NF filter is generally thinner and more uniform which allows CO_2 molecules to pass through quickly.
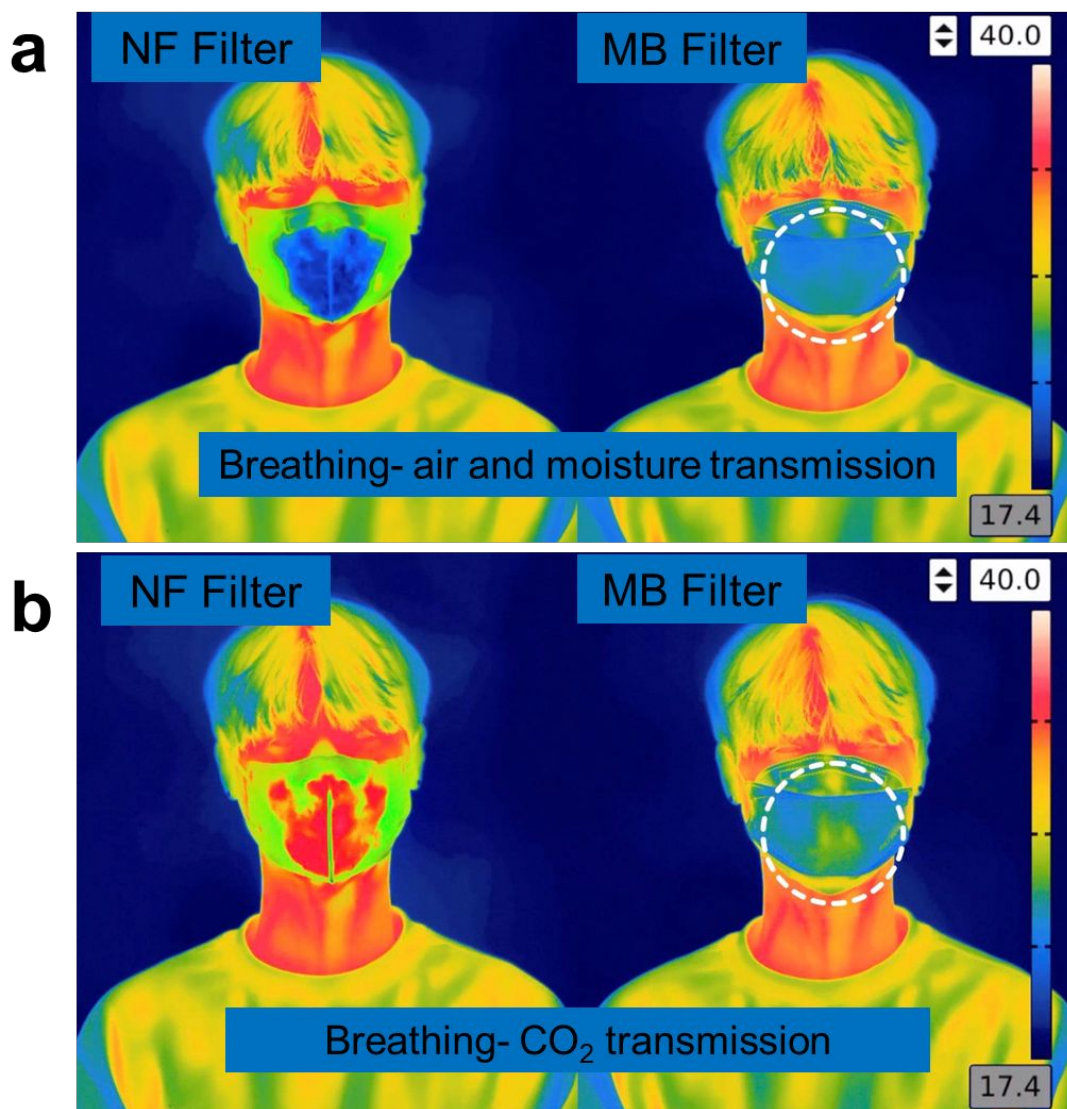
Figure 6 Evaluation of breathing comfort by infrared thermal camera: (a) air and moisture transmission and (b) CO_2 transmission

Evaluation on the surface and morphological property changes

Morphological property changes of both filter types were examined before and after treatment with

75% ethanol (both spraying and dipping treatments). First, through SEM analyses, it was

confirmed that there was no significant change in morphology of the NF filter regardless of ethanol

treatment (**Figure 7a**). NF filter had a uniform morphology without any beads formation during

14

the electrospinning process. The diameter range for all nanofibrous samples was found to be uniform with a narrow diameter distribution. It was interesting to observe that there were no morphological changes of nanofibers even after 24 h dipping time and 10 cycle spraying. In the case of MB filter, it was clearly observed non-uniform morphology with a wide range of diameters (**Figure 7a**). Diameters of MB fibers were found to be from sub-microns to tens of microns. Also, there were no alignments in fibers. However, the MB filter was also found to be morphological consistent when treated with ethanol. Magnified SEM images with clear scale bar can be viewed in supplementary material (Figure S1 (a , b))

Next, surface area change was analyzed after ethanol treatment. As expected, MB filter exhibited much lower surface area (average of 0.588 $m^2 g^{-1}$), while it was increased according to treatment time (**Figure 7b**); the MB filter with ethanol treatment for 24 h presented a 3-fold higher surface area than the non-treated sample. The same phenomena were also observed for the NF filter. Its high surface area (average of 12.529 $m^2 g^{-1}$) was also increased with increasing treatment time. In the case of MB filter, surface area might increase due to shrinkage of individual fibers on exposure to ethanol (but, it was not clearly observed in SEM images, might be too less to be observed). In the case of the NF filter, the depolymerization of the thinning spun-bond PET layer can be a reason for the increasing trend of surface area. Because this was not the main objective of this study, we do not claim any possible reactions in this work.

Porosities of both types of filters were calculated before and after both types of treatments (**Figure 7c**). MB filter exhibited higher porosity (as visually its looked like a sponge) than NF filter. It was also observed that the porosity of both types of filters displayed an increasing trend with increasing treatment time. Porosities of these filters were also reflected in the results of air permeability and pressure drop.
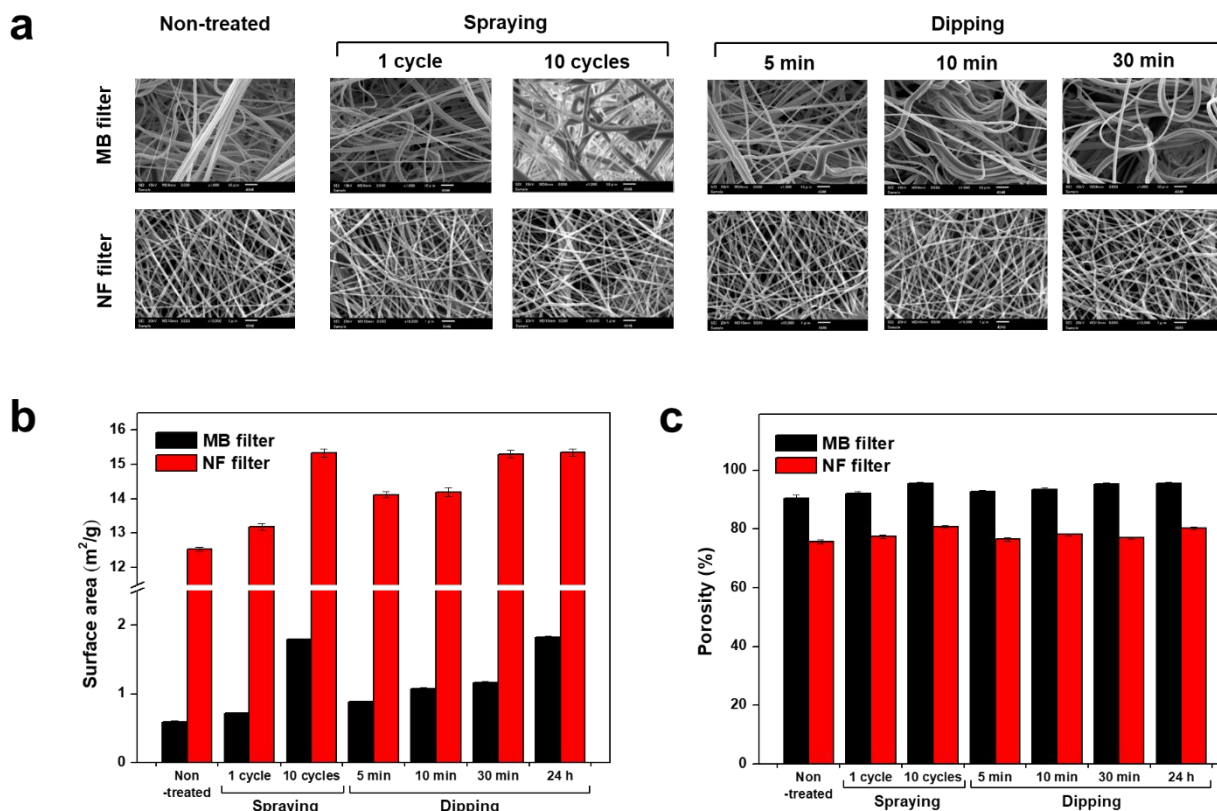
Figure 7 (a) SEM images, (b) surface area, and (c) porosity of MB and NF face mask filters before and after spraying and dipping treatments. SEM images were taken at a magnification of 1,000 for MB filter and 10,000 for NF filter. The lengths of scale bars are 10 μm for MB filter and 1 μm for NF filter.

Hydrophilic or The hydrophobic nature of the filter surface also plays an important role in providing favorable or unfavorable environments to different types of bacteria and viruses. (21) Moisture retaining property is also dependent on the hydrophilic nature of the substrate. Thus, water contact angles of both filters were determined before and after ethanol treatments (**Figure 8**). It was observed that water contact angles of both filter types were recorded above 90°, indicating that both filters are hydrophobic in nature. In particular, the NF surface had a much larger water contact angle above 150°, which can be considered as a super-hydrophobic surface. However, there was a slight increase in the water contact angle of MB filter when treated with

16

ethanol and it might be due to decreased static surface charge. The water contact angle for the NF

filter was slightly decreased after treatment with ethanol due to possible degradation of ester

linkages in PET as described in porosity measurement. Importantly, in any treatment conditions,

both filters are still in the range of hydrophobicity (> 90°). (40) Thus, it was considered that the

mechanical and chemical properties of both filter materials were not significantly changed by

ethanol treatment. The face mask should prevent wetting by moisture and saliva splash to prohibit

not only pathogen transmission, but also bacterial growth inside. (45,46)
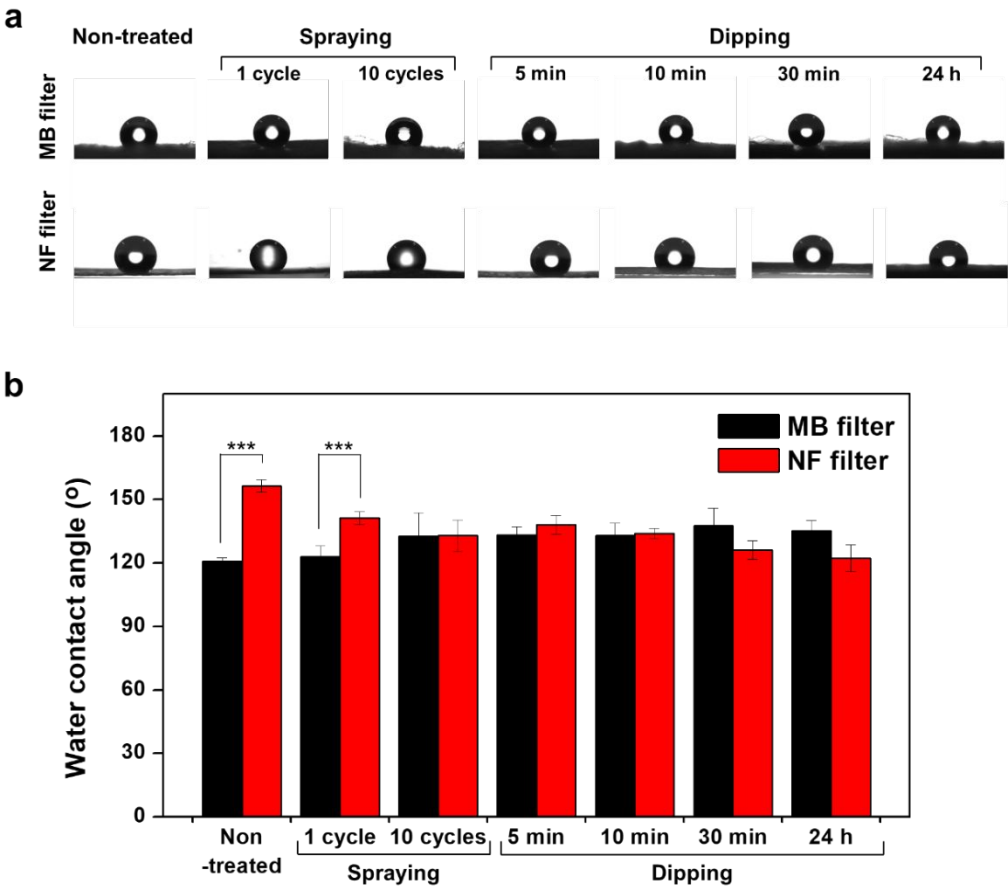

Figure 8 (a) Images of water droplets on contacted surfaces and (b) calculated contact angles of MB and NF face mask filters before and after spraying and dipping treatments. The values and error bars represent the means ± standard deviations of at least 5 samples with statistical significance from unpaired t-test (***p < 0.005).

Evaluation of antibacterial efficiency of ethanol treatment

Because ethanol plays an antibiotic role in contaminated microorganisms, (47) antibacterial efficiencies of ethanol treatment process on filters were evaluated. Bacterial cells spread on the filter surface were treated with 75% ethanol and cultured in liquid medium for 12 h. As a result, we found that optical densities of cultured both filters were dramatically decreased when filters were treated with ethanol spraying or dipping process **(Figure 9)**. In particular, spraying with 1 cycle (3 times press) or dipping for 5 min was enough for complete suppression of bacterial growth on both filter types. Thus, it was concluded that simple ethanol treatments are sufficient for an antibacterial effect on both MB and NF filter types.

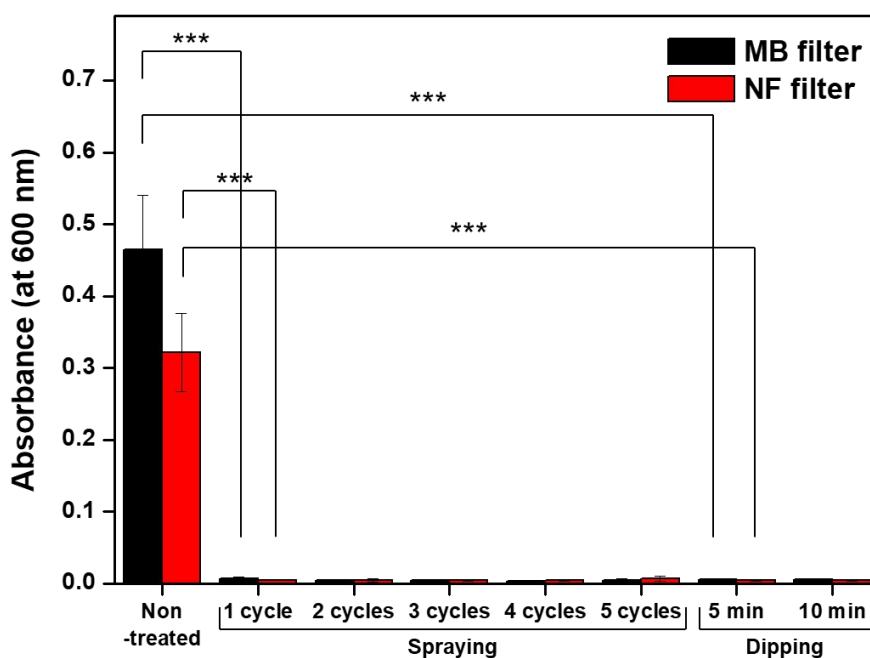**Figure 9** Sterilization efficiency of bacterial cells-loaded MB and NF face mask filters before and after spraying and dipping treatments. The samples were incubated in LB media at 37 ℃ for 12 h and the remaining cells were quantified by measuring optical density. The values and error bars represent the means ± standard deviations of at least 6 samples with statistical significance from unpaired t-test (***$p < 0.005$).

Evaluation of filter cytocompatibility

Human keratinocyte HaCaT and endothelial HUVEC cells were selected to consider possible

exposure of face mask filter material to face skin and respiratory system. (48,49) As a result, both

filter types did not have cytotoxicity to HaCaT cells under all given conditions (**Figure 10a**).

However, in the case of the MB filter, the viability of HUVEC cells was significantly decreased

with over 1.5% (w/v) filter extract concentration. According to ISO 10993-5, the relative cell

viability above 80% is discriminated to be not cytotoxic at the condition, while the viability within

80-60% is weak, 60-40% is moderate, and 40-0% is strong cytotoxic. (50) Notably, the NF filter

did not have cytotoxicity for both human cell types. These results were also confirmed through

live/dead fluorescence microscopic analyses (**Figure 10b**). Thus, it was concluded that both filters

will be harmless to face skin contact while MB filter might have somewhat toxicity to vascular

cells. These might be due to the growth condition of the vascular endothelium is more demanding

than that of skin keratinocyte.
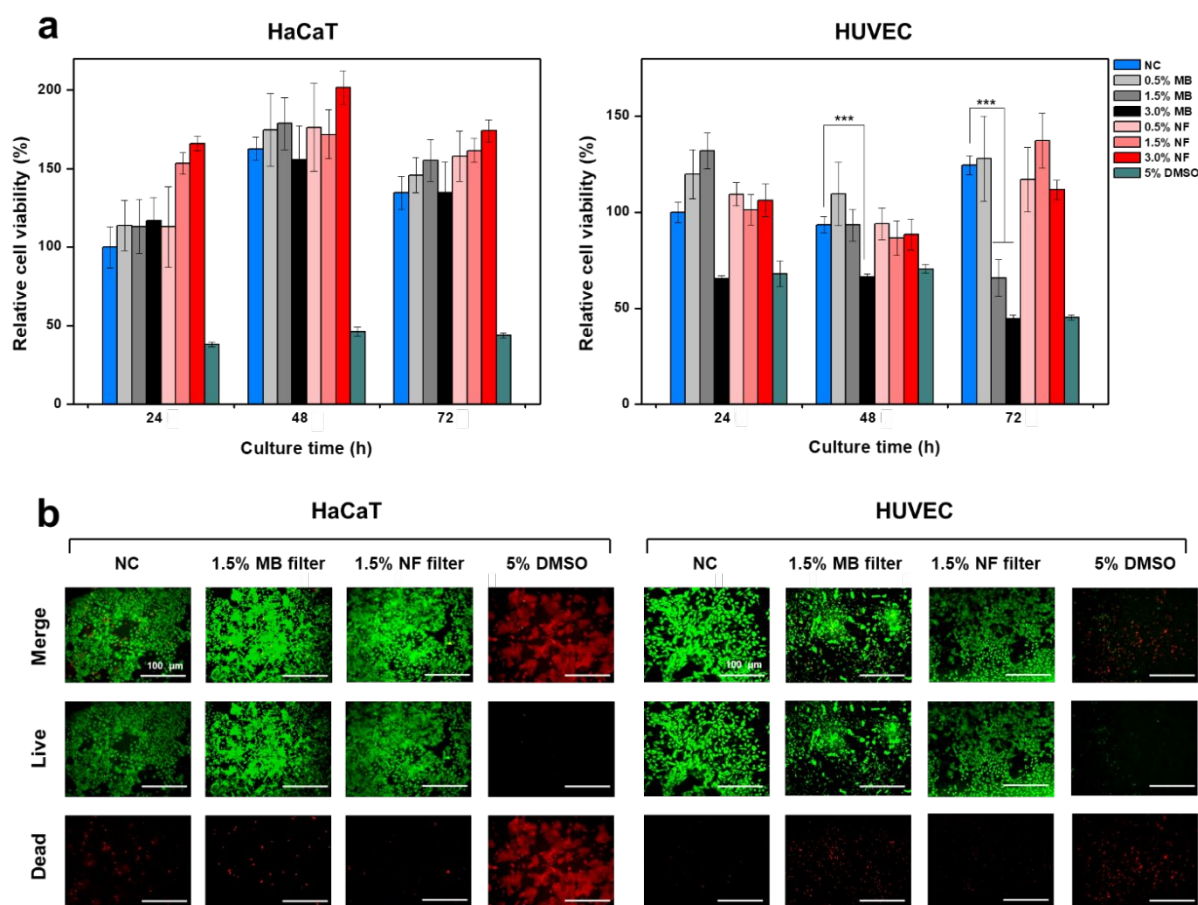
Figure 10 Cytocompatibility of MB and NF face mask filters before and after spraying and dipping treatments. (a) Relative cell viability of HaCaT and HUVEC cells by CCK-8 assay and (b) live/dead fluorescent cell images at 72 h culture. The length of each scale bar is 100 μm. Blank medium and 5% DMSO were used as negative control (NC) and positive control, respectively. The values and error bars represent the means ± standard deviations of at least 5 samples with statistical significance from unpaired t-test (***p < 0.005).

Conclusions

Considering several filter performance parameters, the reusability of the face mask is the need of the hour. Especially, due to the shortage of face masks around the globe in COVID-19 pandemic, it is highly desired to find a way to reuse face mask with minimum chances of risk. Here, we performed a comparative evaluation on the reusability of two types of face mask filters using

simple ethanol cleaning method including spraying and dipping. MB filter exhibited better air permeability (as twice as that of NF filter) before and after treatment by ethanol and it can be associated with higher porosity of MB filter which was recorded as high as ~96%. NF filter had lower porosity (< ~80%) and this can also be directly associated with pressure drop which was higher (up to 183 Pa) before and after treatment with ethanol. Because of good air permeability, pressure drop, and morphological properties regardless of ethanol treatment, both filter types qualify the basic criteria of face mask application. However, considering the filtration efficiency aspect, while the MB filter will be effective for single use only due to its prompt reduction to ~64% by ethanol cleaning, the NF filter might be valid for multiple reuses due to its very consistent (~97-99%) efficiency. In addition, the NF filter did not show cytotoxicity to the tested human cells. Thus, by considering all the comparative evaluations, it can be concluded that while both MB and NF filters have similar filtration performance for single-use applications, MB filter cannot be reused as its filtration efficiency drops drastically and NF filter can be successfully reused for multiple times after simple cleaning with ethanol.

Methods

Material selection and cleaning procedures

Melt blown polypropylene (PP) is often used as filter for face masks. However, polyvinylidene difluoride ((PVDF) (electrospun or melt blown)) is not commonly used as filter of mask. We selected PVDF as nanofibrous filter for face mask because of its smoother morphology, uniform pore structure, and good bonding ability with spun bond PET. Although, other polymers (PAN, PVA, etc.) can also be used as electrospun nanofibers for filter applications but every polymer has its limitations. Polypropylene (PP) based MB filter (in N95 face mask) was purchased from the market and electrospun polyvinylidene difluoride (PVDF) based NF filter supported by spun bond

polyethylene terephthalate (PET) was provided from Lemon Corporation (Gumi, Korea). Composition (w/w) of NF filter was as follows; PET:PVDF = 98:2. MB and NF-based nonwoven filters were cleaned with two types of treatments: spraying of 75% ethanol with 1-10 cycles (1 cycle is 3 times press) and dipping in 75% ethanol for 5 min-24 h (**Figure 1**). All samples were air-dried prior to characterization. Then, performance parameters including air permeability, pressure drop, filtration efficiency, and surface and morphological properties were comparatively evaluated.

Characterization of performance parameters

The filter samples were characterized by scanning electron microscope (SEM; JSM-5300; JEOL Ltd, Japan) to observe the potential change in their structural morphology. Surface area analysis was performed using Brunauer-Emmett-Teller (BET; Tristar II 3020; Shimadzu, Japan). Air permeability analysis was performed using Lab Air IV (FX3300; area, 38 cm^2@125Pa; TextTest Instruments, Switzerland) to measure airflow rates of the filters. Filtration efficiency analysis was also performed using an automatic filter scanner (AFS153; aerosol, DEHS@0.3mm; area, 100 cm^2@32LPM; Topas GmbH, Germany) for estimation of reuse time. Differential pressure drop was also investigated using AFS153 (area, 100 cm^2@32LPM). An air flow of 32 L/min, was opted for air permeability and pressure drop tests, which is standard air flow rate for normal human breathing. Breathing comfort and thermal behavior of wearing face masks were evaluated using an infrared thermal camera (Fotric 226; FOTRIC, China). Breathability test was performed using upright cup method (A-2). Samples were prepared following ASTM E 96. (51) Water vapor transport rate (also used as moisture vapor transport rate MVTR) WVTR was calculated for each specimen.

22

For measuring porosity, filter mats were cut into 4×4 cm^2 of a rectangle shape and subsequently weighed. The filter thickness was measured using a digital thickness gauge at five different places and averaged out for further calculations. The apparent volume (Va) was measured using the dimensions of the previously cut filter mat. The volume (Vg) was determined by the density of the PET (1.38 g cm^{-3}), PP (0.94 g cm^{-3}) and PVDF (1.78 g cm^{-3}) and their weight ratio in the respective specimen. Porosity was calculated using the following equation as below

$$Porosity\ \% \ = 1 - \frac{Vg}{Va} X\ 100$$ Equation 1 porosity measurement

For determining the water contact angle, the filter samples were cut into 2×7 cm^2 of a rectangle shape. Fully air-dried filters were placed on a microscope slide, and 3 μL of distilled water was dropped on the filter surface through a 23-gauge blunt needle tip. Photograph of each water droplet on the filter was acquired and analyzed by Smartdrop (Femtobiomed, Korea). The average of the left and right angles was taken as the water contact angle.

Antibacterial activity analyses

Bacterial dispersion solution was prepared by culturing *Escherichia coli* cells in a liquid medium of 20 g/L Luria-Bertani (LB) broth (Sigma-Aldrich, USA) at 37 ℃. The solution was transferred to spray bottle when its optical density at 600 nm (OD$_{600}$) reached to ~1, and sprayed onto filters by pressing 3 times. After ethanol treatment and sufficient air drying, the filters were cut into 1×1 cm^2 of a rectangle shape and soaked in 0.5 mL of LB medium at 48-well cell culture plates. After 12 h culturing at 37 ℃, the OD$_{600}$ of each medium was measured to configure the survival of the bacterial cells in the filters.

Cytocompatibility analyses

Human keratinocyte (HaCaT) cells and human umbilical vein endothelial (HUVEC; Lonza, Swiss) cells were used for evaluation of cytocompatibility of MB and NF filters. Dulbecco's modified Eagle's medium (DMEM; HyClone) was used for HaCaT cell culture and EGM-2 BulletKit (Lonza) was used for HUVEC cell culture. Each filter extract was prepared by incubating filter in cell culture medium at 37 ℃ for 24 h according to ISO 10993-5. (50) Pre-cultured cells were seeded in 96-well cell culture plate (SPL Life Science, Korea) to a density of 1×10^4 per each well with 100 µL medium, and cultured in a humid incubator with 5% CO_2 at 37 ℃. After 24 h, the medium was exchanged to the same amount of medium containing filter extract of 0.5, 1.5, and 3.0 % (w/v) and further cultured for 24, 48, and 72 h. Black medium and 5% (v/v) dimethyl sulfoxide (DMSO) were compared as negative and positive controls, respectively. Cell viability was quantitatively determined using the Cell Counting Kit-8 assay (CCK-8; Dojindo, Japan). To visualize cytocompatibility, the cells after 72 h culture were dyed by LIVE/DEAD Viability/Cytotoxicity Kit (Thermo Fisher Scientific, USA). After 30 min reaction with light-blocking, the sample was observed by a fluorescence microscope (BX60; Olympus, Japan). Calcein-acetoxymethyl ester penetrated into the cytosol of live cells exhibits green light, while ethidium homodimer emits red light penetrating into the nucleus of dead cells. The image was acquired and merged by iSolution (IMT i-Solution Inc., Korea).

Acknowledgement

Conflict of interest

Authors declare no conflict of interest in this research.

References

(1)   World Health Organization, COVID-19 Global situation https://who.sprinklr.com/.

(2)   Wang, D.; Hu, B.; Hu, C.; Zhu, F.; Liu, X.; Zhang, J.; Wang, B.; Xiang, H.; Cheng, Z.; Xiong, Y.; Zhao, Y.; Li, Y.; Wang, X.; Peng, Z. Clinical Characteristics of 138 Hospitalized Patients with 2019 Novel Coronavirus-Infected Pneumonia in Wuhan, China. *JAMA - J. Am. Med. Assoc.* **2020**, *323* (11), 1061–1069. https://doi.org/10.1001/jama.2020.1585.

(3)   Guan, W.; Ni, Z.; Hu, Y.; Liang, W.; Ou, C.; He, J.; Liu, L.; Shan, H.; Lei, C.; Hui, D. S. C.; Du, B.; Li, L.; Zeng, G.; Yuen, K.-Y.; Chen, R.; Tang, C.; Wang, T.; Chen, P.; Xiang, J.; Li, S.; Wang, J.; Liang, Z.; Peng, Y.; Wei, L.; Liu, Y.; Hu, Y.; Peng, P.; Wang, J.; Liu, J.; Chen, Z.; Li, G.; Zheng, Z.; Qiu, S.; Luo, J.; Ye, C.; Zhu, S.; Zhong, N. Clinical Characteristics of Coronavirus Disease 2019 in China. *N. Engl. J. Med.* **2020**, 1–13. https://doi.org/10.1056/nejmoa2002032.

(4)   Holshue, M. L.; DeBolt, C.; Lindquist, S.; Lofy, K. H.; Wiesman, J.; Bruce, H.; Spitters, C.; Ericson, K.; Wilkerson, S.; Tural, A.; Diaz, G.; Cohn, A.; Fox, L. A.; Patel, A.; Gerber, S. I.; Kim, L.; Tong, S.; Lu, X.; Lindstrom, S.; Pallansch, M. A.; Weldon, W. C.; Biggs, H. M.; Uyeki, T. M.; Pillai, S. K. First Case of 2019 Novel Coronavirus in the United States. *N. Engl. J. Med.* **2020**, *382* (10), 929–936. https://doi.org/10.1056/NEJMoa2001191.

25

(5) Chan, J. F. W.; Yuan, S.; Kok, K. H.; To, K. K. W.; Chu, H.; Yang, J.; Xing, F.; Liu, J.; Yip, C. C. Y.; Poon, R. W. S.; Tsoi, H. W.; Lo, S. K. F.; Chan, K. H.; Poon, V. K. M.; Chan, W. M.; Ip, J. D.; Cai, J. P.; Cheng, V. C. C.; Chen, H.; Hui, C. K. M.; Yuen, K. Y. A Familial Cluster of Pneumonia Associated with the 2019 Novel Coronavirus Indicating Person-to-Person Transmission: A Study of a Family Cluster. *Lancet* **2020**, *395* (10223), 514–523. https://doi.org/10.1016/S0140-6736(20)30154-9.

(6) Wax, R. S.; Christian, M. D. Practical Recommendations for Critical Care and Anesthesiology Teams Caring for Novel Coronavirus (2019-NCoV) Patients. *Can. J. Anesth.* **2020**. https://doi.org/10.1007/s12630-020-01591-x.

(7) Ivanov, D. Predicting the Impacts of Epidemic Outbreaks on Global Supply Chains: A Simulation-Based Analysis on the Coronavirus Outbreak (COVID-19/SARS-CoV-2) Case. *Transp. Res. Part E Logist. Transp. Rev.* **2020**, *136* (March), 101922. https://doi.org/10.1016/j.tre.2020.101922.

(8) Kampf, G.; Voss, A.; Scheithauer, S. Inactivation of Coronaviruses by Heat. *J. Hosp. Infect.* **2020**, No. PG-. https://doi.org/https://doi.org/10.1016/j.jhin.2020.03.025.

(9) Chen, N.; Zhou, M.; Dong, X.; Qu, J.; Gong, F.; Han, Y.; Qiu, Y.; Wang, J.; Liu, Y.; Wei, Y.; Xia, J.; Yu, T.; Zhang, X.; Zhang, L. Epidemiological and Clinical Characteristics of 99 Cases of 2019 Novel Coronavirus Pneumonia in Wuhan, China: A Descriptive Study. *Lancet* **2020**, *395* (10223), 507–513. https://doi.org/10.1016/S0140-6736(20)30211-7.

(10) Li, Q.; Guan, X.; Wu, P.; Wang, X.; Zhou, L.; Tong, Y.; Ren, R.; Leung, K. S. M.; Lau, E. H. Y.; Wong, J. Y.; Xing, X.; Xiang, N.; Wu, Y.; Li, C.; Chen, Q.; Li, D.; Liu, T.; Zhao, J.; Liu, M.; Tu, W.; Chen, C.; Jin, L.; Yang, R.; Wang, Q.; Zhou, S.; Wang, R.; Liu, H.; Luo, Y.; Liu, Y.; Shao, G.; Li, H.; Tao, Z.; Yang, Y.; Deng, Z.; Liu, B.; Ma, Z.; Zhang, Y.; Shi,

G.; Lam, T. T. Y.; Wu, J. T.; Gao, G. F.; Cowling, B. J.; Yang, B.; Leung, G. M.; Feng, Z. Early Transmission Dynamics in Wuhan, China, of Novel Coronavirus-Infected Pneumonia. *N. Engl. J. Med.* **2020**, *382* (13), 1199–1207. https://doi.org/10.1056/NEJMoa2001316.

(11)   Zhu, N.; Zhang, D.; Wang, W.; Li, X.; Yang, B.; Song, J.; Zhao, X.; Huang, B.; Shi, W.; Lu, R.; Niu, P.; Zhan, F.; Ma, X.; Wang, D.; Xu, W.; Wu, G.; Gao, G. F.; Tan, W. A Novel Coronavirus from Patients with Pneumonia in China, 2019. *N. Engl. J. Med.* **2020**, *382* (8), 727–733. https://doi.org/10.1056/NEJMoa2001017.

(12)   Zhou, P.; Yang, X. Lou; Wang, X. G.; Hu, B.; Zhang, L.; Zhang, W.; Si, H. R.; Zhu, Y.; Li, B.; Huang, C. L.; Chen, H. D.; Chen, J.; Luo, Y.; Guo, H.; Jiang, R. Di; Liu, M. Q.; Chen, Y.; Shen, X. R.; Wang, X.; Zheng, X. S.; Zhao, K.; Chen, Q. J.; Deng, F.; Liu, L. L.; Yan, B.; Zhan, F. X.; Wang, Y. Y.; Xiao, G. F.; Shi, Z. L. A Pneumonia Outbreak Associated with a New Coronavirus of Probable Bat Origin. *Nature* **2020**, *579* (7798), 270–273. https://doi.org/10.1038/s41586-020-2012-7.

(13)   Li, P.; Fu, J.-B.; Li, K.-F.; Chen, Y.; Wang, H.-L.; Liu, L.-J.; Liu, J.-N.; Zhang, Y.-L.; Liu, S.-L.; Tang, A.; Tong, Z.-D.; Yan, J.-B. Transmission of COVID-19 in the Terminal Stage of Incubation Period: A Familial Cluster. *Int. J. Infect. Dis.* **2020**. https://doi.org/10.1016/j.ijid.2020.03.027.

(14)   Leung, N. H. L.; Chu, D. K. W.; Shiu, E. Y. C.; Chan, K.-H.; McDevitt, J. J.; Hau, B. J. P.; Yen, H.-L.; Li, Y.; Ip, D. K. M.; Peiris, J. S. M.; Seto, W.-H.; Leung, G. M.; Milton, D. K.; Cowling, B. J. Respiratory Virus Shedding in Exhaled Breath and Efficacy of Face Masks. *Nat. Med. 2020* **2020**, 1–5. https://doi.org/10.1038/s41591-020-0843-2.

(15)   Wu, H.; Huang, J.; Zhang, C. J. P.; He, Z.; Ming, W.-K. Facemask Shortage and the Novel

Coronavirus Disease (COVID-19) Outbreak: Reflections on Public Health Measures. *EClinicalMedicine* **2020**, *000*, 100329. https://doi.org/10.1016/j.eclinm.2020.100329.

(16)   Lowe, J. J.; Paladino, K. D.; Farke, J. D.; Boulter, K.; Cawcutt, K.; Emodi, M.; Hankins, R.; Hinkle, L.; Micheels, T.; Schwedhelm, S.; Vasa, A.; Watson, S.; Rupp, M. E. N95 Filtering Facepiece Respirator Ultraviolet Germicidal Irradiation (UVGI) Process for Decontamination and Reuse. **2020**.

(17)   Lee, S.; Cho, A. R.; Park, D.; Kim, J. K.; Han, K. S.; Yoon, I.-J.; Lee, M. H.; Nah, J. Reusable Polybenzimidazole Nanofiber Membrane Filter for Highly Breathable PM2.5 Dust Proof Mask. *ACS Appl. Mater. Interfaces* **2019**, *11* (3), 2750–2757. https://doi.org/10.1021/acsami.8b19741.

(18)   Lin, T. H.; Chen, C. C.; Huang, S. H.; Kuo, C. W.; Lai, C. Y.; Lin, W. Y. Filter Quality of Electret Masks in Filtering 14.6–594 Nm Aerosol Particles: Effects of Five Decontamination Methods. *PLoS One* **2017**, *12* (10), 1–15. https://doi.org/10.1371/journal.pone.0186217.

(19)   Konda, A.; Prakash, A.; Moss, G. A.; Schmoldt, M.; Grant, G. D.; Guha, S. Aerosol Filtration Efficiency of Common Fabrics Used in Respiratory Cloth Masks. *ACS Nano* **2020**. https://doi.org/10.1021/acsnano.0c03252.

(20)   Li, Y.; Tokura, H.; Guo, Y. P.; Wong, A. S. W.; Wong, T.; Chung, J.; Newton, E. Effects of Wearing N95 and Surgical Facemasks on Heart Rate, Thermal Stress and Subjective Sensations. *Int. Arch. Occup. Environ. Health* **2005**, *78* (6), 501–509. https://doi.org/10.1007/s00420-004-0584-4.

(21)   Li, Y.; Wong, T.; Chung, J.; Guo, Y. P.; Hy, J. Y.; Guan, Y. T.; Yao, L.; Song, Q. W.; Newton, E. In Vivo Protective Performance of N95 Respirator and Surgical Facemask. *Am.*

J. Ind. Med. **2006**, *49* (12), 1056–1065. https://doi.org/10.1002/ajim.20395.

(22)   Bałazy, A.; Toivola, M.; Adhikari, A.; Sivasubramani, S. K.; Reponen, T.; Grinshpun, S.
        A. Do N95 Respirators Provide 95% Protection Level against Airborne Viruses, and How
        Adequate Are Surgical Masks? *Am. J. Infect. Control* **2006**, *34* (2), 51–57.
        https://doi.org/10.1016/j.ajic.2005.08.018.

(23)   Lim, E. C. H.; Seet, R. C. S.; Lee, K. H.; Wilder-Smith, E. P. V.; Chuah, B. Y. S.; Ong, B.
        K. C. Headaches and the N95 Face-Mask amongst Healthcare Providers. *Acta Neurol.
        Scand.* **2006**, *113* (3), 199–202. https://doi.org/10.1111/j.1600-0404.2005.00560.x.

(24)   Loeb, M.; Dafoe, N.; Mahony, J.; John, M.; Sarabia, A.; Glavin, V.; Webby, R.; Smieja,
        M.; Earn, D. J. D.; Chong, S.; Webb, A.; Walter, S. D. Surgical Mask vs N95 Respirator for
        Preventing Influenza among Health Care Workers: A Randomized Trial. *JAMA - J. Am.
        Med. Assoc.* **2009**, *302* (17), 1865–1871. https://doi.org/10.1001/jama.2009.1466.

(25)   Kharaghani, D.; Gitigard, P.; Ohtani, H.; Kim, K. O.; Ullah, S.; Saito, Y.; Khan, M. Q.;
        Kim, I. S. Design and Characterization of Dual Drug Delivery Based on In-Situ Assembled
        PVA/PAN Core-Shell Nanofibers for Wound Dressing Application. *Sci. Rep.* **2019**, *9* (1),
        1–11. https://doi.org/10.1038/s41598-019-49132-x.

(26)   Ullah, S.; Hashmi, M.; Kharaghani, D.; Khan, M. Q.; Saito, Y.; Yamamoto, T.; Lee, J.;
        Kim, I. S. Antibacterial Properties of in Situ and Surface Functionalized Impregnation of
        Silver Sulfadiazine in Polyacrylonitrile Nanofiber Mats. *Int. J. Nanomedicine* **2019**, *14*,
        2693–2703. https://doi.org/10.2147/IJN.S197665.

(27)   Hashmi, M.; Ullah, S.; Kim, I. S. Electrospun Momordica Charantia Incorporated Polyvinyl
        Alcohol (PVA) Nanofibers for Antibacterial Applications. *Mater. Today Commun.* **2020**,
        101161. https://doi.org/https://doi.org/10.1016/j.mtcomm.2020.101161.

(28) Ullah, A.; Ullah, S.; Khan, M. Q.; Hashmi, M.; Nam, P. D.; Kato, Y.; Tamada, Y.; Kim, I. S. Manuka Honey Incorporated Cellulose Acetate Nanofibrous Mats: Fabrication and in Vitro Evaluation as a Potential Wound Dressing. *Int. J. Biol. Macromol.* **2020**, *155*, 479–489. https://doi.org/10.1016/j.ijbiomac.2020.03.237.

(29) Ullah, S.; Hashmi, M.; Khan, M. Q.; Kharaghani, D.; Saito, Y.; Yamamoto, T.; Kim, I. S. Silver Sulfadiazine Loaded Zein Nanofiber Mats as a Novel Wound Dressing. *RSC Adv.* **2019**, *9* (1), 268–277. https://doi.org/10.1039/C8RA09082C.

(30) Khan, M. Q.; Kharaghani, D.; Nishat, N.; Ishikawa, T.; Ullah, S.; Lee, H.; Khatri, Z.; Kim, I. S. The Development of Nanofiber Tubes Based on Nanocomposites of Polyvinylpyrrolidone Incorporated Gold Nanoparticles as Scaffolds for Neuroscience Application in Axons. *Text. Res. J.* **2018**, 004051751880118. https://doi.org/10.1177/0040517518801185.

(31) Ullah, S.; Hashmi, M.; Hussain, N.; Ullah, A.; Sarwar, M. N.; Saito, Y.; Kim, S. H.; Kim, I. S. Stabilized Nanofibers of Polyvinyl Alcohol (PVA) Crosslinked by Unique Method for Efficient Removal of Heavy Metal Ions. *J. Water Process Eng.* **2020**, *33* (December 2019), 101111. https://doi.org/10.1016/j.jwpe.2019.101111.

(32) Hashmi, M.; Ullah, S.; Kim, I. S. Copper Oxide (CuO) Loaded Polyacrylonitrile (PAN) Nanofiber Membranes for Antimicrobial Breath Mask Applications. *Curr. Res. Biotechnol.* **2019**, *1* (1), 1–10. https://doi.org/10.1016/j.crbiot.2019.07.001.

(33) Chen, Y.; Amiri, A.; Boyd, J. G.; Naraghi, M. Promising Trade-Offs Between Energy Storage and Load Bearing in Carbon Nanofibers as Structural Energy Storage Devices. *Adv. Funct. Mater.* **2019**, *29* (33), 1–11. https://doi.org/10.1002/adfm.201901425.

(34) Morent, R.; De Geyter, N.; Leys, C.; Gengembre, L.; Payen, E. Comparison between XPS-

And FTIR-Analysis of Plasma-Treated Polypropylene Film Surfaces. *Surf. Interface Anal.* **2008**, *40* (3–4), 597–600. https://doi.org/10.1002/sia.2619.

(35)   Shen, Y.; Wu, P. Two-Dimensional ATR-FTIR Spectroscopic Investigation on Water Diffusion in Polypropylene Film: Water Bending Vibration. *J. Phys. Chem. B* **2003**, *107* (18), 4224–4226. https://doi.org/10.1021/jp0269975.

(36)   Liu, X. D.; Sheng, D. K.; Gao, X. M.; Li, T. B.; Yang, Y. M. UV-Assisted Surface Modification of PET Fiber for Adhesion Improvement. *Appl. Surf. Sci.* **2013**, *264*, 61–69. https://doi.org/10.1016/j.apsusc.2012.09.107.

(37)   Wei, Y.; Chu, H. Q.; Dong, B. Z.; Li, X.; Xia, S. J.; Qiang, Z. M. Effect of TiO2 Nanowire Addition on PVDF Ultrafiltration Membrane Performance. *Desalination* **2011**, *272* (1–3), 90–97. https://doi.org/10.1016/j.desal.2011.01.013.

(38)   Madaeni, S. S.; Zinadini, S.; Vatanpour, V. A New Approach to Improve Antifouling Property of PVDF Membrane Using in Situ Polymerization of PAA Functionalized TiO2 Nanoparticles. *J. Memb. Sci.* **2011**, *380* (1–2), 155–162. https://doi.org/10.1016/j.memsci.2011.07.006.

(39)   Rahimpour, A.; Jahanshahi, M.; Rajaeian, B.; Rahimnejad, M. TiO2 Entrapped Nano-Composite PVDF/SPES Membranes: Preparation, Characterization, Antifouling and Antibacterial Properties. *Desalination* **2011**, *278* (1–3), 343–353. https://doi.org/10.1016/j.desal.2011.05.049.

(40)   De Castro, R. E. N.; Vidotti, G. J.; Rubira, A. F.; Muniz, E. C. Depolymerization of Poly(Ethylene Terephthalate) Wastes Using Ethanol and Ethanol/Water in Supercritical Conditions. *J. Appl. Polym. Sci.* **2006**, *101* (3), 2009–2016. https://doi.org/10.1002/app.23748.

(41) Fernandes, J. Rodrigues; Amaro, L. Pereira; Muniz, E. Curti; Favaro, S. L.; Radovanovic, E. PET Depolimerization in Supercritical Ethanol Conditions Catalysed by Nanoparticles of Metal Oxides. *J. Supercrit. Fluids* **2020**, *158*, 104715. https://doi.org/https://doi.org/10.1016/j.supflu.2019.104715.

(42) Kim, J.-H.; Roberge, R. J.; Powell, J. B.; Shaffer, R. E.; Ylitalo, C. M.; Sebastian, J. M. Pressure Drop of Filtering Facepiece Respirators: How Low Should We Go? *Int. J. Occup. Med. Environ. Health* **2015**, *28* (1), 71–80. https://doi.org/10.13075/ijomeh.1896.00153.

(43) Kilic, A.; Shim, E.; Pourdeyhimi, B. Electrostatic Capture Efficiency Enhancement of Polypropylene Electret Filters with Barium Titanate. *Aerosol Sci. Technol.* **2015**, *49* (8), 666–673. https://doi.org/10.1080/02786826.2015.1061649.

(44) Guy, J. S.; Breslin, J. J.; Breuhaus, B.; Vivrette, S.; Smith, L. G. Characterization of a Coronavirus Isolated from a Diarrheic Foal. *J. Clin. Microbiol.* **2000**, *38* (12), 4523–4526. https://doi.org/10.1128/jcm.38.12.4523-4526.2000.

(45) Wang, N.; Cai, M.; Yang, X.; Yang, Y. Electret Nanofibrous Membrane with Enhanced Filtration Performance and Wearing Comfortability for Face Mask. *J. Colloid Interface Sci.* **2018**, *530*, 695–703. https://doi.org/10.1016/j.jcis.2018.07.021.

(46) Ekabutr, P.; Chuysinuan, P.; Suksamrarn, S.; Sukhumsirichart, W.; Hongmanee, P.; Supaphol, P. Development of Antituberculosis Melt-Blown Polypropylene Filters Coated with Mangosteen Extracts for Medical Face Mask Applications. *Polym. Bull.* **2019**, *76* (4), 1985–2004. https://doi.org/10.1007/s00289-018-2468-x.

(47) Yoo, J.-H. Review of Disinfection and Sterilization – Back to the Basics. *Infect. Chemother.* **2018**, *50* (2), 101. https://doi.org/10.3947/ic.2018.50.2.101.

(48) Cao, Y.; Gong, Y.; Liu, L.; Zhou, Y.; Fang, X.; Zhang, C.; Li, Y.; Li, J. The Use of Human

Umbilical Vein Endothelial Cells (HUVECs) as an in Vitro Model to Assess the Toxicity of Nanoparticles to Endothelium: A Review. *J. Appl. Toxicol.* **2017**, *37* (12), 1359–1369. https://doi.org/10.1002/jat.3470.

(49)   López-García, J.; Lehocký, M.; Humpolíček, P.; Sáha, P. HaCaT Keratinocytes Response on Antimicrobial Atelocollagen Substrates: Extent of Cytotoxicity, Cell Viability and Proliferation. *J. Funct. Biomater.* **2014**, *5* (2), 43–57. https://doi.org/10.3390/jfb5020043.

(50)   ISO 10993-5:2009 Biological Evaluation of Medical Devices. Part 5: Tests for In Vitro Cytotoxicity. International Organization for Standardization; Geneva, Switzerland.

(51)   ASTM E96 Standard Test Methods for Water Vapor Transmission of Shipping Containers —. **2003**, *95* (Reapproved), 4–6. https://doi.org/10.1520/D4279-95R09.2.